

Spreen, G., L. Kaleschke, and G. Heygster: "Operational Sea Ice Remote Sensing with AMSR-E 89 GHz Channels", 2005 IEEE International Geoscience and Remote Sensing Symposium Proceedings, IEEE, 6, 4033 - 4036, 2005.

©2005 IEEE. Personal use of this material is permitted. However, permission to reprint/republish this material for advertising or promotional purposes or for creating new collective works for resale or redistribution to servers or lists, or to reuse any copyrighted component of this work in other works must be obtained from the IEEE.



# Operational Sea Ice Remote Sensing with AMSR-E 89 GHz Channels

(Invited Paper)

Gunnar Spreen  
Centre of Marine and  
Atmospheric Sciences  
University of Hamburg  
Bundesstr. 53, 20146 Hamburg  
Germany  
Email: spreen@ifm.zmaw.de

Lars Kaleschke  
Institute of Environmental Physics  
University of Bremen  
P.O. Box 330440, 28334 Bremen  
Germany  
Email: lkalesch@iup.physik.uni-bremen.de

Georg Heygster  
Institute of Environmental Physics  
University of Bremen  
P.O. Box 330440, 28334 Bremen  
Germany  
Email: heygster@uni-bremen.de

**Abstract**—Recent progress in spatial resolution enhancement of sea ice concentrations obtained by microwave remote sensing has been stimulated by two new developments: First, the new sensors AMSR (Advanced Microwave Scanning Radiometer) on MIDORI-II and AMSR-E on AQUA offer horizontal resolutions of 6x4 km at 89 GHz. This is nearly three times the resolution of the standard sensor SSM/I at 85 GHz (15x13 km). The sampling distance at the high frequencies is 12.5 km at SSM/I and 5 km at the AMSR-E instrument. Second, a new algorithm enables the estimation of sea ice concentrations from the channels near 90 GHz, despite the enhanced atmospheric influence in these channels. This allows to fully exploit their horizontal resolution which is two to three times finer than the one of the channels near 19 and 37 GHz. These frequencies are used by the most widespread algorithms for sea ice retrieval, the NASA Team and Bootstrap algorithms. These two developments are combined to determine operationally sea ice concentration maps. The used ASI (Artist Sea Ice) algorithm combines a model for retrieving the sea ice concentration from SSM/I 85 GHz data proposed by Svendsen et al. [1] with an ocean mask derived from the 18-, 23-, and 37-GHz AMSR-E data using two weather filters and the Bootstrap Algorithm. The AMSR-E sea ice concentration data are projected into grids of sampling sizes down to 3 km. Hemispherical and regional maps are provided daily at [www.iup.physik.uni-bremen.de](http://www.iup.physik.uni-bremen.de).

## I. INTRODUCTION

Sea ice concentrations, i.e. the covered percentage of a given area with sea ice, are retrieved by passive microwave sensors since the start of the ESMR (Electrically Scanning Microwave Radiometer) sensor in December 1972. Since 1987 the SSM/I (Special Sensor Microwave/Imager) is widely used for sea ice concentration determination. A restriction of this instruments is the coarse resolution of the data.

In 2002 two new microwave radiometers were launched. AMSR-E (Advanced Microwave Scanning Radiometer for EOS) on the AQUA platform and AMSR (Advanced Microwave Scanning Radiometer) on the MIDORI-II (formerly ADEOS-II) satellite. Control over MIDORI-II was lost in October 2003. Therefore only AMSR-E data is used here.

The main advantage of AMSR-E in comparison to SSM/I is its improved spatial resolution. For the 89 GHz channels used here the resolution is improved by factor 3 in comparison

to SSM/I 85 GHz channels (SSM/I footprint size: 13x15 km<sup>2</sup>, AMSR-E footprint size: 4x6 km<sup>2</sup>). The resolution of ice concentrations derived using the widespread NASA Team and Bootstrap sea ice concentration algorithms is restricted by the channels involved with the lowest resolution, i.e. the 19 GHz channels, that is 43x69 km<sup>2</sup> for SSM/I and 16x27 km<sup>2</sup> for AMSR-E. Thus the here presented sea ice concentrations represent an improvement in spatial resolution of more than a factor of 3 compared to non-89 GHz sea ice concentrations.

## II. ARTIST SEA ICE ALGORITHM

The here used ARTIST Sea Ice (ASI) algorithm was originally developed to benefit from the high spatial resolution of the 85 GHz channels of the SSM/I sensor [2]. It is an enhancement of the Svendsen sea ice algorithm for frequencies near 90 GHz [1]. One advantage of the ASI algorithm in contrast to other 85 GHz algorithms is that it solely bases on one instrument and does not need additional data sources as input. It shows a similar performance as other sea ice algorithms [3].

The ASI algorithm distinguishes water and ice by the value of the polarization difference  $P$  of the brightness temperatures  $T_B$ ,

$$P = T_{B,V} - T_{B,H} \quad (1)$$

with  $V$  for vertical and  $H$  for horizontal polarization. It is known from surface measurements that the polarization difference of the emissivity is similar for all ice types and much smaller than for open water (Fig. 1). As the temperature of the ocean near the ice is almost constant at  $-1.8^\circ\text{C}$  and the temperature of the ice is not varying very much this is also true for the polarization difference  $P$ . For the influence of the atmosphere on the polarization difference we have

$$P = P_s e^{-\tau} (1.1 e^{-\tau} - 0.11) = P_s a_i \quad (2)$$

with opacity  $\tau$  and surface polarization difference  $P_s$ . This approximation is applicable for a horizontally stratified atmosphere under arctic conditions with an effective constant temperature and a diffusely reflecting surface viewed under an incident angle of approximately  $50^\circ$  [1]. Then the polarization

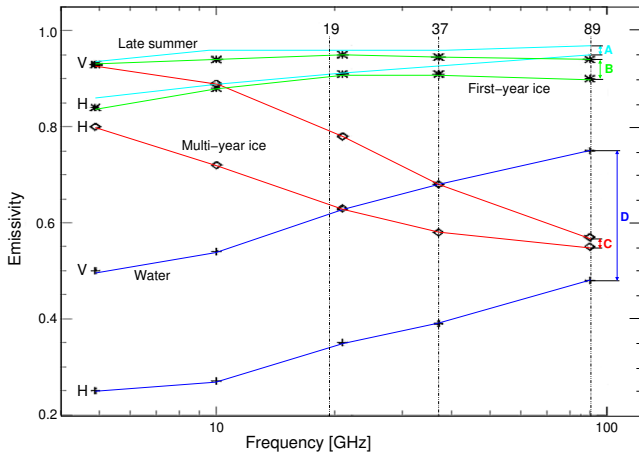


Fig. 1. Vertical (V) and horizontal (H) emissivity of sea ice and sea water measured under an incident angle of  $\theta = 50^\circ$  in winter and summer. At 89 GHz the emissivity differences A, B and C for the different ice types are similar and much smaller than the emissivity difference D of water.

difference in dependence of the ice concentration  $C$  can be written as

$$P = (C P_{s,i} + (1 - C) P_{s,w}) a_i \quad (3)$$

with  $P_{s,i}$  and  $P_{s,w}$  as surface polarization differences for ice and water, respectively. The atmospheric influence  $a_i$  is a function of the ice concentration [1]. With (3) the polarization difference  $P_0$  for the ice concentration  $C = 0$  (open water) and atmospheric influence  $a_0$  is given by

$$P_0 = a_0 P_{s,w} \quad (4)$$

and similarly for the ice concentration  $C = 1$  (closed ice cover) by

$$P_1 = a_1 P_{s,i} \quad (5)$$

Taylor expansion of equation 3 around  $C = 0$  and  $C = 1$  gives

$$P = a_0 C(P_{s,i} - P_{s,w}) + P_0 \quad \text{for } C \rightarrow 0 \quad (6)$$

$$P = a_1 (C - 1)(P_{s,i} - P_{s,w}) + P_1 \quad \text{for } C \rightarrow 1. \quad (7)$$

if all higher terms are neglected and  $a'_0$  and  $a'_1$  considered to be zero. With equations (4) and (5) the dependence of the atmospheric influence can be substituted and the ice concentration is given by:

$$C = \left( \frac{P}{P_0} - 1 \right) \left( \frac{P_{s,w}}{P_{s,i} - P_{s,w}} \right) \quad \text{for } C \rightarrow 0 \quad (8)$$

$$C = \frac{P}{P_1} + \left( \frac{P}{P_1} - 1 \right) \left( \frac{P_{s,w}}{P_{s,i} - P_{s,w}} \right) \quad \text{for } C \rightarrow 1. \quad (9)$$

For Arctic conditions  $\left( \frac{P_{s,w}}{P_{s,i} - P_{s,w}} \right) = -1.14$  is a typical value for sea ice signatures [1]. To be able to retrieve all ice concentration values between 0% and 100% we need to interpolate between the solutions (8) and (9). Assuming the atmospheric influence to be a smooth function of  $C$  we select a third order polynomial for the sea ice concentration between open water and 100% ice cover:

$$C = d_3 P^3 + d_2 P^2 + d_1 P + d_0. \quad (10)$$

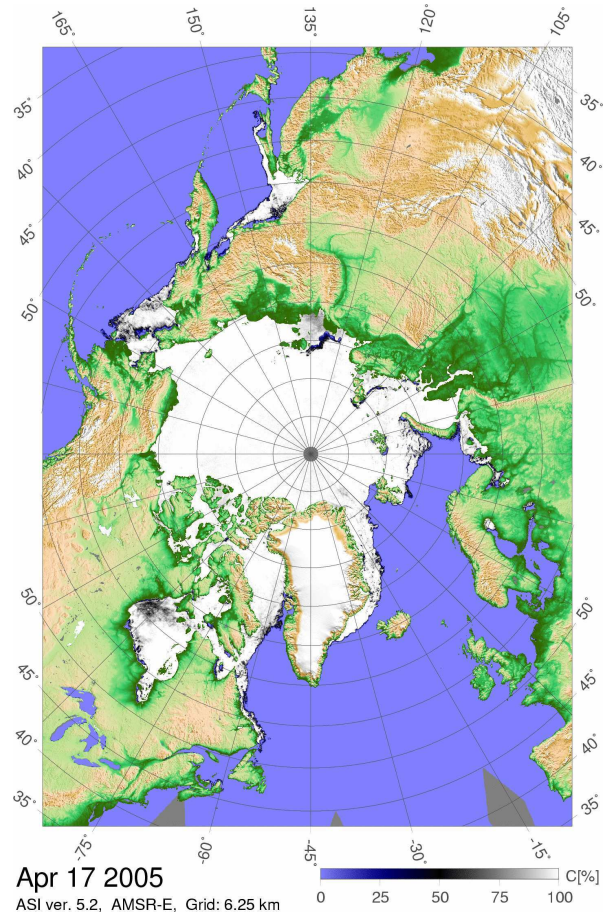


Fig. 2. Arctic sea ice concentration map of Apr-17-2005 calculated from AMSR-E data using the ASI algorithm. In contrast to the scientific color table of Fig. 3 a more intuitive color table is used to visualize the ice concentrations for non scientific users.

With (8) and (9) and their first derivatives the unknowns  $d_i$  in (10) can be determined. Then (10) can be used to calculate the sea ice concentration if the tie-points  $P_0$  and  $P_1$  for open water and 100% ice coverage are known.

The correct choice of the tie-points is important for the retrieval of the sea ice concentration as they also include the overall atmospheric influence. The ASI algorithm uses fixed tie-points found by comparing ice concentrations of the Svendsen algorithm with well calibrated reference ice concentrations. They can for example be obtained from the lower frequency channels of the radiometer which suffer less from the atmospheric influence.

Effective filters are necessary to remove spurious ice concentrations in open water areas. The weather filtering process consists of three steps. All of them are using the lower frequency channels with lower spatial resolution. This does not lead to a lower resolved ice edge of the ASI data [2] but it may cause pixels along the ice edge to show too high ice concentrations due to missing weather filters.

*a)* : The first weather filter uses the gradient ratio (GR) of the 36.5 and 18.7 GHz channels [4] which is positive for water but near zero or negative for ice. This ratio mainly

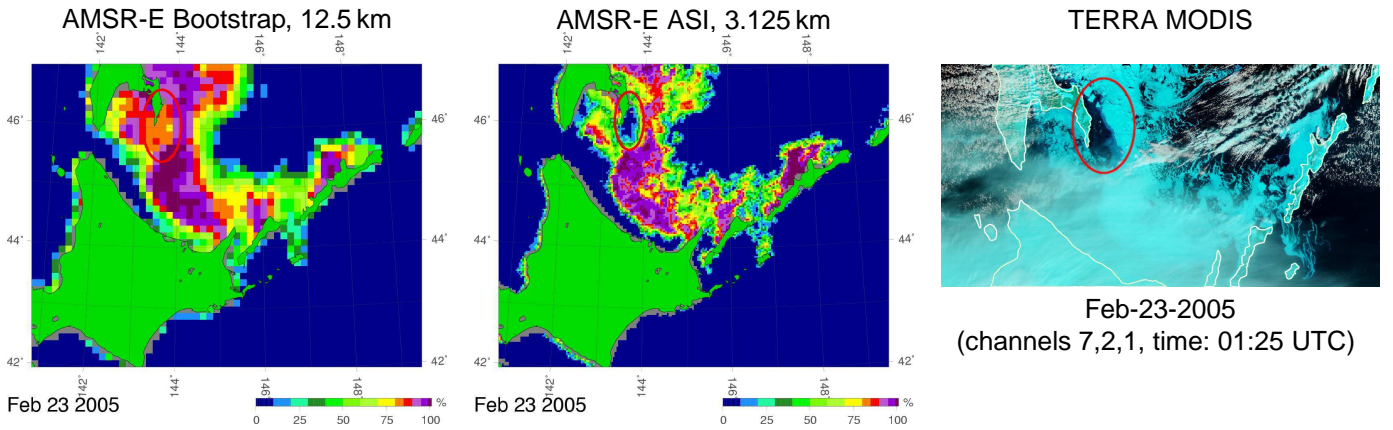


Fig. 3. Comparison of ice concentrations on Feb-23-2005 in the Sea of Okhotsk. The left image shows the Bootstrap ice concentrations in a 12.5 km grid which matches the spatial resolution of the data. The middle image shows the ASI ice concentrations in a 3.125 km grid. The red ellipse marks a region of open water which is clearly visible in the ASI ice concentrations and the MODIS false color image of that day (right image) but is not visible in the Bootstrap data due to the lower resolution.

filters high cloud liquid water cases. Fourteen scatter plots  $GR(36.5/18.7)$  vs. the 18.7 GHz polarization ratio distributed over all seasons and both hemispheres were analyzed to find an optimal threshold which does not filter out too many low ice concentrations but cuts off all spurious ice:  $GR(36.5/18.7) \geq 0.045 \Rightarrow C(ASI) = 0$ . This threshold at least keeps all ice concentrations above 15% which often is defined as the ice edge contour line.

b) : To additionally exclude high water vapor cases above open water the gradient ratio  $GR(23.8/18.7)$  is used [5] and by a study similar to a) a second threshold was found as  $GR(23.8/18.7) \geq 0.04 \Rightarrow C(ASI) = 0$ .

c) : Finally all ASI ice concentration data with corresponding Bootstrap ice concentration data below 5% are set to zero:  $C(Bootstrap) \leq 5\% \Rightarrow C(ASI) = 0$ . After applying these filters only very few extreme weather events may still cause spurious ice in the open ocean.

A sea ice concentration map showing the complete Arctic on a 6.25 km grid and using the tie-points  $P_0 = 47\text{K}$  and  $P_1 = 11.7\text{K}$  is shown in Fig. 2. These maps are operationally published by the IUP, University Bremen ([www.iup.physik.uni-bremen.de](http://www.iup.physik.uni-bremen.de)) on a daily base using the data of the day before.

An example of the accomplished improvements in the spatial resolution in comparison to the Bootstrap algorithm is demonstrated in the Sea of Okhotsk (Fig. 3) where a fraction of open water evolved along the south-easterly end of Sakhalin. A region of open water can be clearly identified in the MODIS false color image (Fig. 3 right) of that day. It is correctly reproduced in the ASI AMSR-E ice concentrations (middle), but not in the Bootstrap AMSR-E one (left). The coarse resolution of the 18.7 ( $\approx 20.1\text{ km}$ ) and 36.5 GHz ( $\approx 10.6\text{ km}$ ) channels used for the Bootstrap algorithm and all other low frequency algorithm totally smears out the open water.

### III. VALIDATION AND ERROR ESTIMATION

The tie-point  $P_0$  and  $P_1$  determine the maximum and minimum polarization difference, respectively. All polarization

differences above (below)  $P_0$  ( $P_1$ ) are set to 0% (100%) ice concentration. The atmospheric influence on  $P_1$  can be neglected and all ice types even for different seasons have a similar polarization difference (Fig. 1).  $P_1$  therefore has to be the best representation for all ice types in the dataset. The atmospheric influence on  $P_0$  is much larger. Thus the choice of  $P_0$  also includes the general atmospheric influence on the brightness temperatures.

The time span and region for which a set of tie-points is valid depends on the variability of the atmospheric conditions and the accuracy of the sea ice concentration required for the application at hand.

A 30 days comparison during the Arctic Radiation and Turbulence Interaction Study (ARTIST) of ASI SSM/I ice concentrations with fixed tie-points with those calculated with the NASA Team algorithm [6] showed a mean difference of only  $(1 \pm 4)\%$  [2]. It is therefore not necessary to change the tie-points day by day to get dependable results. This finding is also supported by experiences of the Arctic Ocean Section expedition [7] and the Polarstern ARK-XX/2 expedition from July to August, 2004 when ASI AMSR-E ice concentrations were processed on board.

For the operational ice maps published in the internet a set of constant tie-points is used through the whole year and for both hemispheres to guarantee consistent ice concentrations from day to day. The tie-points  $P_0 = 47\text{K}$ ,  $P_1 = 11.7\text{K}$  have been chosen by correlation comparison with AMSR-E Bootstrap ice concentrations. For regional studies adjusted tie-points may yield better results. For example a different set of tie-points was used during Polarstern expedition ARK-XX/2 ( $P_0 = 50.0$ ,  $P_1 = 9.0$ ) which visually better represented the ice concentrations around the ship as seen by helicopter surveys.

To estimate the errors introduced to the ASI results by the variability of the opacity  $\tau$  and of the surface polarization differences  $P_{s,w}$  and  $P_{s,i}$ , variabilities measured during the ship campaigns NORSEX and MIZEX are used [1]:

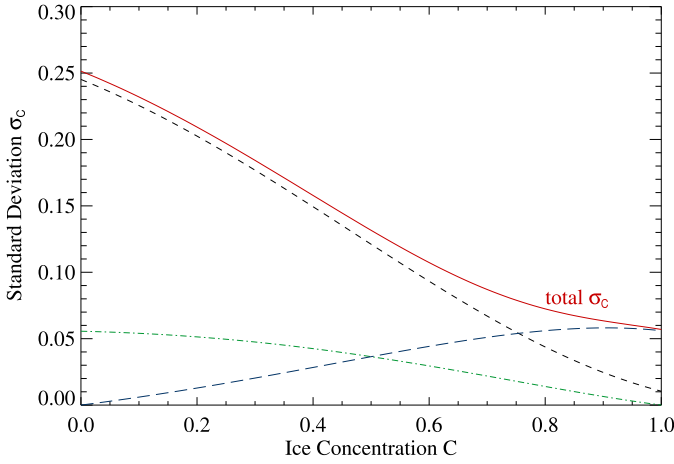


Fig. 4. The expected standard deviation of the ASI ice concentration  $C$  using fixed tie-points and standard deviations of  $\tau$  and  $P_s$  obtained during field measurements. The red curve shows the total expected standard deviation (black dashed: using only  $\sigma_\tau$ , green dash-dotted: only  $\sigma_{P_{s,w}}$ , blue dashed: only  $\sigma_{P_{s,i}}$ ).

$$P_{s,w} = (82 \pm 4) \text{ K} \quad P_{s,i} = (10 \pm 4) \text{ K}$$

$$\tau_w = 0.27 \pm 0.1 \quad \tau_i = 0.14 \pm 0.035.$$

Using (2) the optimal tie-points under these circumstances are found as  $P_0 = 46 \text{ K}$  and  $P_1 = 7.4 \text{ K}$ . They are kept constant and the standard deviation of the ice concentration  $\sigma_C$  in depends of  $C$  is calculated from (3) assuming  $\tau$  to decrease linearly between  $\tau_w$  and  $\tau_i$ . A detailed error analysis [8] (Fig. 4) shows that  $\sigma_C$  decreases from 25% for  $C = 0\%$  to 5.7% for  $C = 100\%$ . Above  $C = 65\%$   $\sigma_C$  is smaller than 10%. This gives an impression about the error introduced through day by day and regional variations of the atmospheric opacity and the surface polarization difference if reliable tie-points are used.

The assumed accuracy of the lower frequency algorithms is approximately 7% but also cases with discrepancies up to 30% have been observed [9]. For high ice concentration values the ASI algorithm fits well into this range. For low ice concentrations the algorithm may significantly overestimate in cases of high cloud liquid water content, especially when cyclones cross the ice edge. On the other hand the 89 GHz channels are less effected by ice types, refrozen meltponds and snow layering, however they are sensitiv to the density and grain size of the snow on top of the sea ice [10].

#### IV. CONCLUSIONS

Today the 89 GHz channels of AMSR-E offer the highest spatial resolution for extraction of daily available, global sea ice concentration data. The ASI ice concentration algorithm uses an empirical model to retrieve the ice concentration between 0% and 100%. It also includes a statistical model about the atmospheric influence. Even if the set of tie-points is not adapted daily for the changing of atmospheric an surface condition, the algorithm shows appropriate results especially at mid and high ice concentrations (above 65%) were the error

should not exceed 10%. In areas with low ice concentrations depending on the atmospheric conditions substantial deviations may occur.

In operational applications this shortcomming generally is more than compensated by the more than 3 times higher spatial resolution of the data in comparison to the conventional passive microwave sea ice concentration algorithms. Systematic sea ice concentration uncertainties affect climate model variables (e.g. the surface air temperature) nearly linearly [11]. However, regional atmospheric models will benefit massively of the increased horizontal resolution of the ice concentration data presented in this study [2].

Additionally the increased resolution reduces the errors due to mixed coastal pixels. This is particular useful when mapping coastal polynyas and smaller seas such as the Baltic Sea, Caspian Sea and the Sea of Okhotsk.

#### ACKNOWLEDGMENT

The authors gratefully acknowledge the support of this work under DFG grants He 1746-10/1,2 and the provision of AMSR-E data by the National Snow and Ice Data center (NSIDC), Boulder, CO, USA. The code of the Bootstrap algorithm has been kindly provided by J. C. Comiso, NASA Goddard Space Flight Center.

#### REFERENCES

- [1] E. Svendsen, C. Mätzler, and T. C. Grenfell, "A model for retrieving total sea ice concentration from a spaceborne dual-polarized passive microwave instrument operating near 90 GHz," *Int. J. Rem. Sens.*, vol. 8, no. 10, pp. 1479–1487, 1987.
- [2] L. Kaleschke, C. Lüpkes, T. Vihma, J. Haarpaintner, A. Bochert, J. Hartmann, and G. Heygster, "SSM/I sea ice remote sensing for mesoscale ocean-atmosphere interaction analysis," *Can. J. Rem. Sens.*, vol. 27, no. 5, pp. 526–537, 2001.
- [3] S. Kern, L. Kaleschke, and D. A. Clausi, "A comparison of two 85 GHz SSM/I ice concentration algorithms with AVHRR and ERS-SAR," *IEEE Trans. Geosci. Rem. Sens.*, vol. 41, no. 10, pp. 2294–2306, 2003.
- [4] P. Gloersen and D. J. Cavalieri, "Reduction of weather effects in the calculation of sea ice concentration from microwave radiances," *J. Geophys. Res.*, vol. 91, no. C3, pp. 3913–3919, 1986.
- [5] D. J. Cavalieri, K. M. St. Germain, and C. T. Swift, "Reduction of weather effects in the calculation of sea-ice concentration with DMSP SSM/I," *J. Glaciology*, vol. 41, no. 139, pp. 455–464, 1995.
- [6] D. J. Cavalieri, P. Gloersen, and W. J. Campbell, "Determination of sea ice parameters with the NIMBUS-7 SMMR," *J. Geophys. Res.*, vol. 89, no. ND4, pp. 5355–5369, 1984.
- [7] L. Lubin, C. Garrity, R. Ramseier, and R. H. Whritner, "Total sea ice concentration retrieval from the SSM/I 85.5 GHz channels during the Arctic summer," *Rem. Sens. Environ.*, vol. 62, no. 1, pp. 63–76, 1997.
- [8] G. Spreen, "Meereisfernerkundung mit dem satellitengestützten Mikrowellenradiometer AMSR(-E) – Bestimmung der Eiskonzentration und Eiskante unter Verwendung der 89 GHz-Kanäle," Diplomarbeit (Master's thesis), University of Hamburg, prepared at the University of Bremen, Dept. of Physics and Electrical Engineering, 2004.
- [9] J. C. Comiso, D. J. Cavalieri, C. L. Parkinson, and P. Gloersen, "Passive microwave algorithms for sea ice concentration: A comparison of two techniques," *Rem. Sens. Environ.*, vol. 60, no. 3, pp. 357–384, 1997.
- [10] R. Tonboe, S. Andersen, L. Toudal, and G. Heygster, "Sea ice emission modelling applications," in *Radiative transfer models for microwave radiometry*, C. Mätzler, Ed. IEE Press Stevenage, Hertfordshire, UK, in press, 2005.
- [11] C. L. Parkinson, D. Rind, R. J. Healy, and D. G. Martinson, "The impact of sea ice concentration accuracies on climate model simulations with the GISS GCM," *J. Climate*, vol. 14, no. 12, pp. 2606–2623, 2001.